Geotechnical Aspects of Underground Construction in Soft Ground – Viggiani (ed)

High-resolution multichannel seismic survey for the excavation of the new headrace tunnel for the Crevola Toce III hydropower scheme in the Ossola Valley, Italy

M. Sapigni
ENEL Produzione S.p.A., Venezia-Mestre, Italy

A.M. Baldi, F. Bianchi & J. De Luca
S.G.G. S.r.l., Siena, Italy

ABSTRACT: A high-resolution seismic survey was conducted for the excavation of the new headrace tunnel for the Crevola Toce III hydropower scheme in an area located between the valleys of the Toce and Diveria rivers. From the geological point of view, the area of the headrace tunnel, 9,2 km long, entirely involves lithotypes belonging to the lower Pennidic Units. In particular the bedrock is composed of a series of gneissic crystalline nappes (Valgrande, Antigorio and Verampio) interlayered by metasediment units (Teggiolo and Baceno) originally corresponding to the triassic-cretaceous sedimentary cover of the crystalline crust. The tunnel path runs mainly through the Antigorio gneiss, but the detailed analysis of the preliminary studies identified a series of geomechanical issues that the tunneling will face through the Baceno metasediments, approximately in the chainage range 6,200–6,700. The metasediments have an average thickness around 70 meters and a general low inclination toward SE; they are composed of a lower gypsum-anhydrite layer locally with micaceous content, fractured marbles and calcschists, and at least two cohesionless sugary carbonate horizons with characteristics of soil. To better define this complex geologic structure, intersected also by a Deep-Seated Gravitational Slope Deformation (DSGSD) with a thickness of 180–260 meters, high resolution seismic reflection and refraction profiles were executed parallel and perpendicular to the tunnel axis, together with VSP and down hole seismic test into geomechanical holes about 400 meters deep drilled near the alignment. In particular, a seismic reflection and refraction line of about 3,000 meters was realized along the tunnel axis. The interpretation of the seismic data through the reflection method, the tomography refraction technique and the tomographic inelastic attenuation processing then allowed geological modelling of the examined area, highlighting the blanket of the DSGSD, its sliding plane, the series of metasediments below, the trends of the basement and also a determination of the geophysics and geomechanics profile along the axis of the tunnel. Based on this data, it was possible to evaluate different tunnel paths aiming to minimize the tunnel length crossing the very poor quality metasedimentary rocks.

Keywords: DSGSD, tunnel, seismic reflection, VSP, seismic refraction, inelastic attenuation, tomography.

1 INTRODUCTION

Seismic reflection data, until recently, has seldom been used for landslide investigations due to the complexity of the internal structure and the relatively rough terrain of landslides. Seismic refraction has been the preferred method in order to supplement geotechnical investigations of landslides consisting of trenching and drilling. However, seismic refraction methods are limited when investigating complex geologic structures with interbedded low- and high-velocity layers.

This study presents the results of a multidisciplinary investigation, centred around seismic reflection profiling, for a new diversion tunnel that will be excavated through a repetition of metamorphic crystalline and sedimentary rocks underlying a prehistoric Deep Seated Gravitational Slope Deformation.

Since the crossing of the metasediments is technically difficult and high risk, a second, more extensive geophysical survey was undertaken with the aim to reconstruct the 3D orientation and thickness of the metasedimentary horizon and the DSGSD basal surface. This would help minimize the tunnel length crossing the very poor quality metasedimentary rocks and maximize the tunnel separation from the overlying deep seated landslide.

2 GEOLOGICAL SETTING

The diversion tunnel layout crosses the deepest part of the Penninic Units traditionally assigned to the ancient northern european margin overthrusted by the oceanic crust and the southern austroalpine margin during the continental collision of the alpine orogenesis. The present-day deep topographic erosion allows us to have a glimpse onto the structure of the Lepontine nappes, tectonic units formed by flat recumbent folds consisting of orthogneissic cores with discontinuous micaschistic and paragneissic outer zones overlaying mesozoic metasediements (Schmidt & Preiswerk 1905; Castiglioni 1958; Milnes et al 1981; Steck, A. 2008). The latter are composed of calcschists, dolomitic and calcitic marbles, quartzites and discontinuous gypsum and anhydritic horizons. This petrographic and rheologic sandwich is the result of many deformative phases the most important of which sliced and thrusted the former continental mainly granitic crust onto the sedimentary cover with displacements of tens of kilometres (Maxelon & Mancktelow; 2005). The amphibolitic metamorphic conditions achieved during the main deformation phase allowed the mineralogical transformations that gave place to the pervasive axial plane foliation forming the present-day schistosity and most prominent weakness planes of the rock mass. Successive slightly or non metamorphic folding events gave the nappe pile its present dominant structure visible along the Antigorio valley with a flat lying attitude in its central part, around the so-called Verampio window, passing to a steep southward inclination near Crevoladossola (Mancktelow N. 1985; Grasemann B., Manktelow N.; 1993) (Fig. 1). The N-S cross section shows the geologic structure of the mountain ridge and the trace of the diversion tunnel. The main feature is represented by the thick, late Variscan (ca. 340 Ma), Antigorio unit composed of a monotonous leucocratic orthogneiss that only rarely shows any structural or petrographic diversity (Bigioggero et al 1977). To the north it overlays the deepest alpine unit corresponding to the equally late variscan Verampio granitic gneiss and its country rock represented by the garnet-rich Baceno micaschists. Interlayered between these two big tectonic units is located the most important permeable unit (Baceno metasediments) which has been well defined after the drilling of three deep boreholes. It has an average thickness around 70 meters and is composed of a lower gypsum-anhydrite layer, at least two cohesionless sugary carbonate horizons, dolomitic marbles and calcschists.

The mountain ridge is cross-cut by many brittle faults arranged in two main sets oriented NW-SE and ENE-WSW. They are the product of the brittle last exhumation phase of the Lepontine dome along the Simplon Fault (Bistacchi & Massironi 2000; Grosjean et al 2004; Zwingmann & Mancktelow, 2004; Campani et al, 2010).

Detailed geological mapping, boreholes and an initial geophysical survey allowed to identify the huge deep seated landslide (DSGSD) (Agliardi et al., 2001) in the northern part of the section that might be genetically linked to the underlying weak metasedimentary horizon. This landslide has a thickness ranging from 180 to 250 m and, under 50–60 m of glacial deposits, it is mainly composed of weak to very weak, degraded Antigorio gneiss. In its northern half the lowermost portion has almost completely involved the metasedimentary layer (Fig. 2).

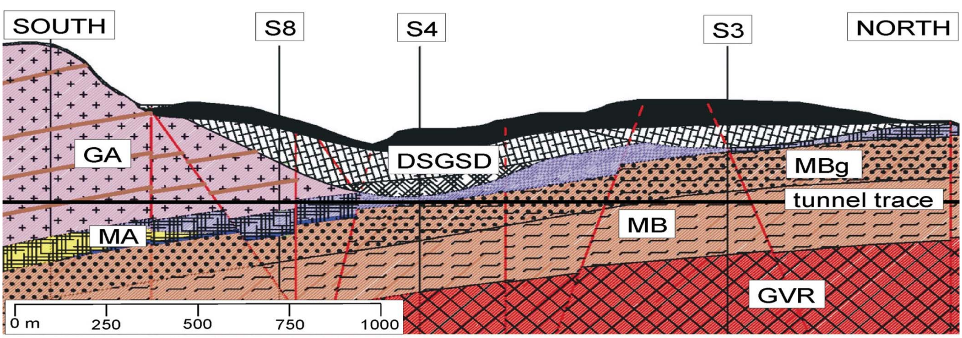

Figure 1. Geological cross section corresponding to the northern half of the diversion tunnel trace. This interpretation was done before the main geophysical survey was performed DSGSD: Deep Seated Gravitational Slope Deformation (involved terrains: black: moraine deposits,light hatch: Antigorio gneiss; heavy hatch: metasediments); GA: Antigorio gneiss; MA: metasediments; MBg: garnet-rich Baceno micaschists; MB: garnet-poor Baceno micaschists; GVR: Verampio gneiss. The location of the three boreholes are also indicated.

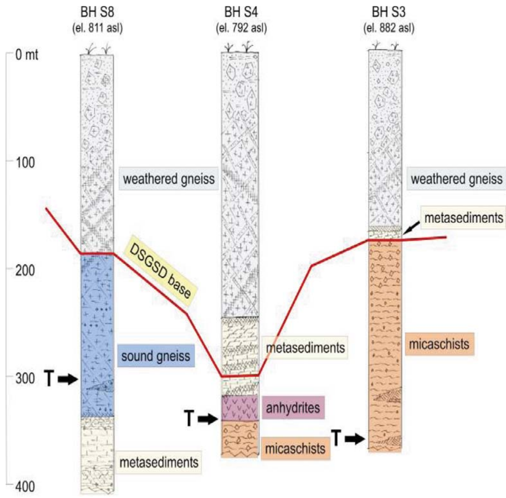

Figure 2. Schematic representation (not to scale) of the main geological units crossed by the boreholes. The horizontal distance between the soundings are: 1,0 km from S3 to S4 and 0,4 km from S4 to S8. T: tunnel elevation.

3 GEOPHYSICAL SURVEY

The principal scope of the geophysical survey was to model the geological structure of the sub-soil in the area between tunnel chainages 4 + 600 and 7 + 600. In this sector, geological and stratigraphic factors had previously not permitted a sufficiently detailed geological modelling.

The geophysical prospecting consisted of the following activities (Fig. 3):

- Seismic reflection profiles (coverage 30 sites over) 6,195 m length;
- Seismic refraction profiles using tomographic method 6,110 m length;
- VSP (Vertical Seismic Profiling) seismic probing in geognostic surveys 525 m length;
- Electrical tomography profiles 1,200 m length.

Seismic reflection profiles were obtained using a nominal coverage of 30 sites, with 120 groups of simultaneously active geophones (4 per group) situated at a distance of 5 metres from each other. Blasting gelatin was used for energization in shafts located at 20 metre intervals.

To record seismic refraction profiles, 120 simultaneously active geophones were utilised and distributed across the soil at a distance of 10 metres from each other. Blasting gelatin was again used for energization in shafts located at 30 metre intervals.

Seismic probing using the V.S.P. method (Vertical Seismic Profiling) was carried out using a chain of 24 geophones at 5 metre intervals, with 2.5 m recording intervals in order to obtain a nominal coverage of 3,000%. With the same scope, seismic velocity measurements were also taken during the surveys, allowing for accurate seismic velocity values to be attributed to the various lithotypes covered by the surveys.

For the analysis of seismic reflection data, the following process was adopted:

Phase 1: Pre-processing

a) Conversation of format
b) Geometry *input*
c) *Trace killing*

Phase 2: Shot data processing

a) RMS *gain*
b) Spectral analysis
c) Band pass pre-filtering
d) Resampling
e) Band pass filtering
f) *Exponential* gain
g) *Mixing*
h) "*Spiking*" deconvolution
i) AGC *gain*
j) *Muting*
k) Band pass filtering
l) *Sorting*

Phase 3: CDP data processing

a) *Pre-stack phase*
   - Aerated static corrections
   - Analysis of velocity every 10 C.D.P.
   - *Normal Moveout* correction
   - Residual static corrections
b) *Stack*
   - C.D.P. summation (stacking)
   - Reduction to common datum
   - RMS *gain*
c) *Post-stack phase*
   - Migration
   - *Mixing*

Phase 4: Complex attributes

Final migrated sections were used to determine complex trace attributes, including instantaneous phase, amplitude envelope and instantaneous frequency (Fig. 4). These parameters are capable of increasing the data's vertical resolution, is particularly the geometrical structure of the reflectors with the instantaneous phase, and variations of signal characteristics on the same reflection with amplitude envelope and instantaneous frequency.

Initially a spectral analysis of the complete set of seismic refraction data was performed in order to verify the frequency distribution of the seismic signal.

The signal was predominantly concentrated at a frequency between 20 and 200 Hz. These values were specified for the band pass filters, to improve the quality and legibility of the seismic data, especially

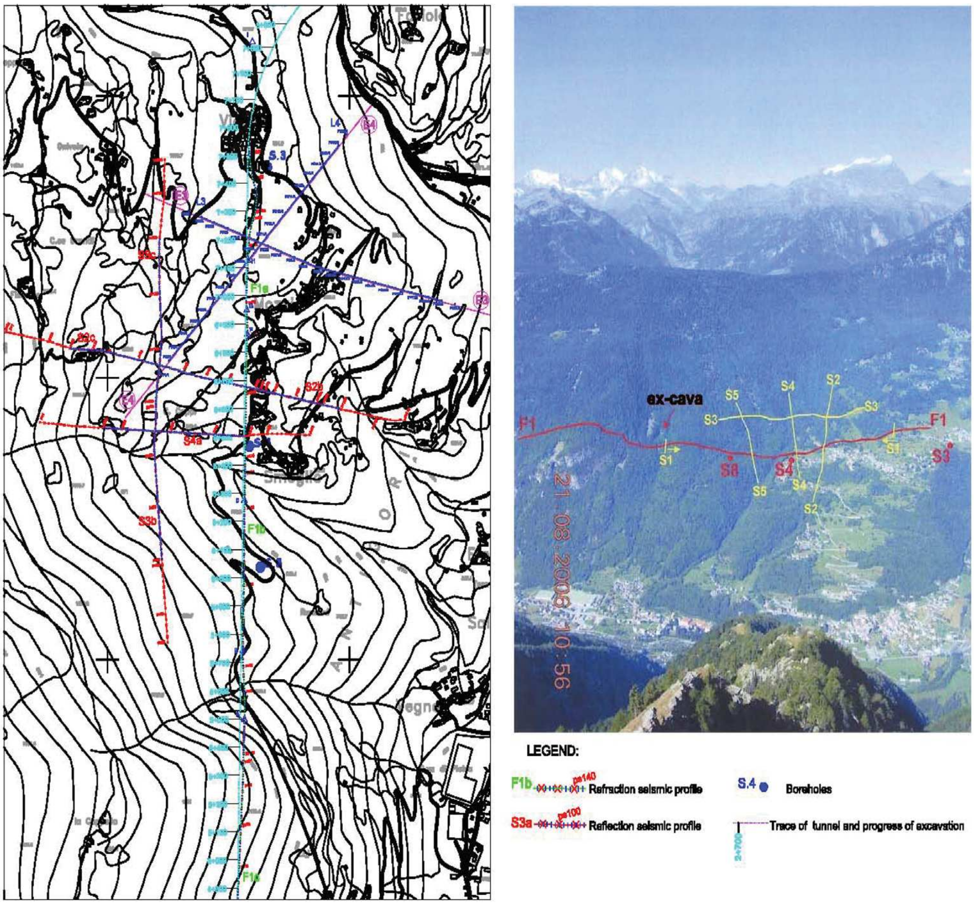

Figure 3. Map and photo of the study area with position of the investigations.

the data derived from distant energization. The tomographic interpretation of seis-mic profiles was carried out using a programme which subdivided the space into 5 m long cells (Fig. 6). Dromocrone graphs for single profiles were interpreted using the G.R.M. method (Generalised Reciprocal Method), used for “reciprocal times”, based on the notion of the delay time of the recorded seismic impulses under the geophones. Such method is characterised by a discrete resolution capacity, and has also proven to be capable of significantly reducing ambiguity caused by the presence of low and/or hidden velocity layers (Fig. 5).

VSPs were obtained at zero offset and proved to be strongly influenced by consistent noise of high amplitude, linked to vertical oscillations of the water column in the surveyed hole. These were most likely associated with the small diameter of the surveyed completion tubing, inside which the chain of geophones acts as a piston. These events and any corresponding events with opposing motion were entirely removed during processing in order to highlight primary reflections, or rather upgoing and even downgoing event types.

4 RESULTS

Using the results of all the seismic profiles made it possible rebuild a 3D geological model of the subsoil. The following maps were prepared to show the geological—geophysical—geomechanical section along the tunnel alignment:

- tectonic model for the area: the fault pattern was developed in two different versions. In the first, fault correlation follows only geophysical and interpretative criteria and is controlled by the planimetric layout of the profiles. In the second version the fault pattern has been modified to better integrate with regional geology.

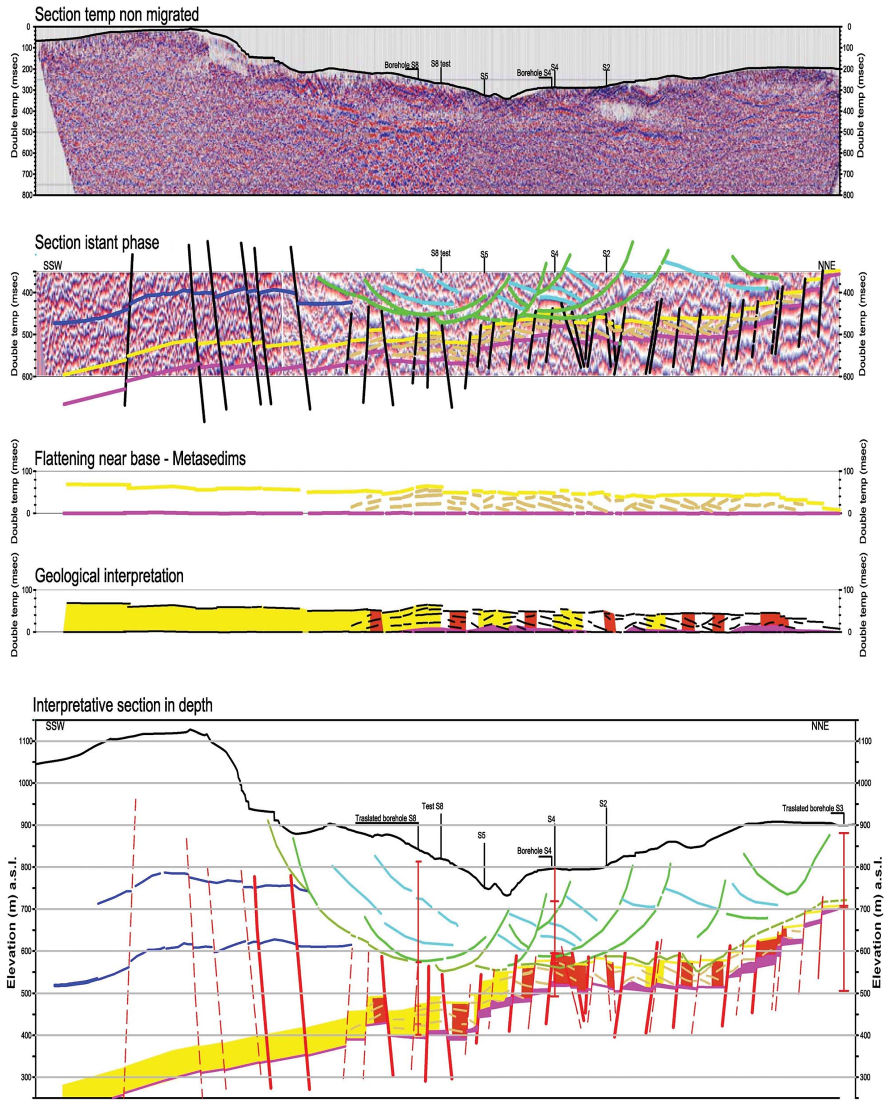

Figure 4. Reflection seismic profile n°1.

- DSGSD bed: stratigraphic results of the three deep seismic surveys carried out using survey adjustment.
- Topographic map of metasedimentary sequence top surface: created using seismic profiles with samples taken at 10 metre intervals.
- Map of the basement top surface: for this plot samples were taken every 10 metres on the seismic profiles. The development of this surface was correlated by a slight emergence in the northern zone, located at 770 m above sea level, showing that the base dips to the south-east. Over the axis of the tunnel approximately two kilometres toward the south, the altitude is approximately 225 m above sea level.
- thickness map of metasedimentary sequence: Samples were taken every 10 metres on the seismic lines. Thickness trends reveal a maximum in the north-western zones, of 125 m and minimum values across the eastern area; the minimum thickness is at deep seismic survey S3.
- Map of compression wave velocity (Vp): seismic velocity values were obtained at the tunnel elevation of 510 m above sea level. These values were attributed to the different cells in the tomographic interpretation, and an isoline map

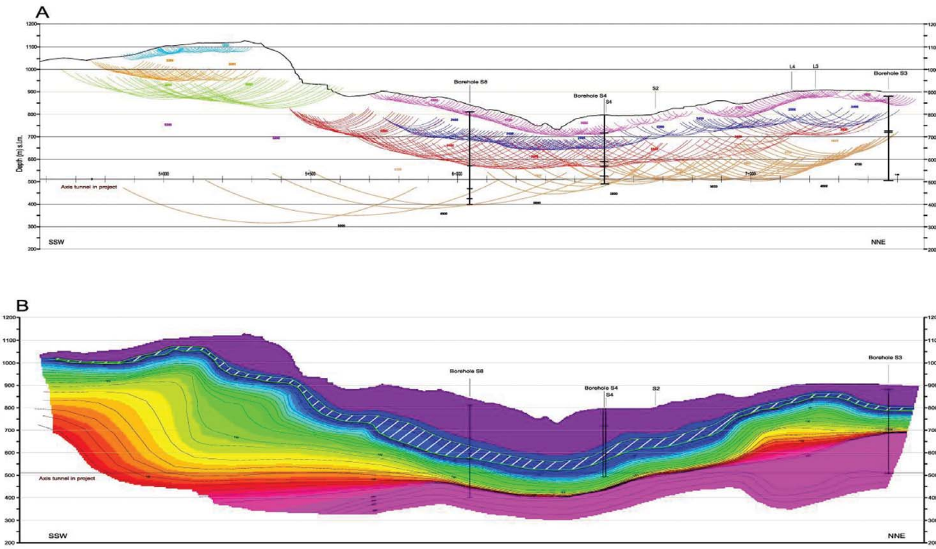

Figure 5. Rifraction seismic profile n°1: A Interpretative Section GRM: B Anaelastic attenuation elaboration.

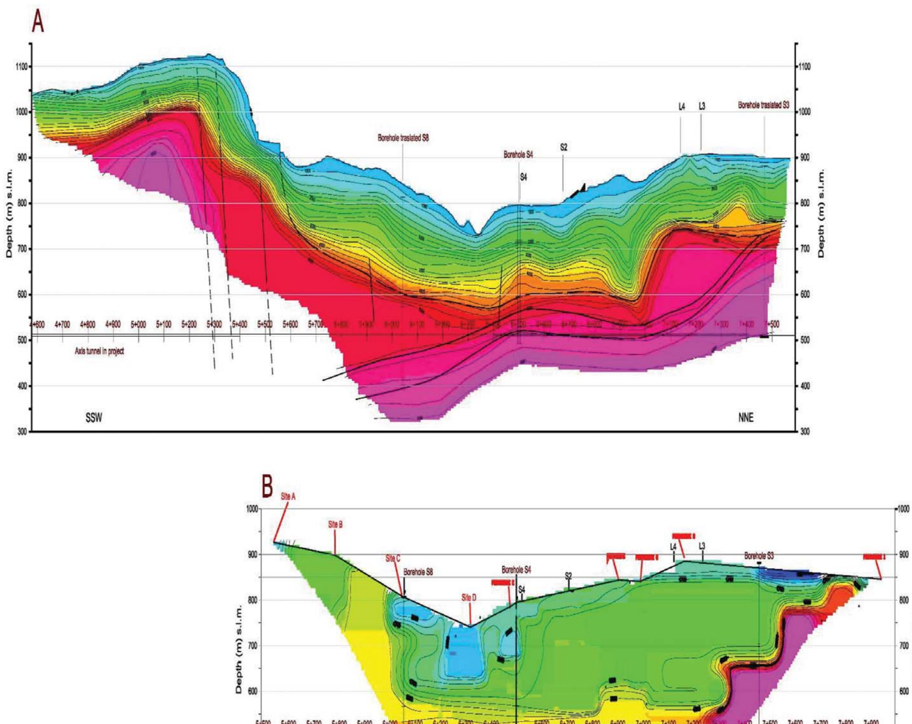

Figure 6. Tomographic analysis of seismic profile 1 integrated with the velocity data of the boreholes (A); Seismic tomography section only from boreholes (B).

was been published. This map shows a rather constant value of Vp to the west of the tunnel, whilst revealing decreasing values of Vp towards the east (towards the valley).

- map of stack seismic velocity: using interval velocity determined on seismic reflection profiles at 510 m above sea level, seismic velocity values were obtained which do not correspond with values obtained using seismic refraction. However the values provide a comprehensive understanding of the resistance characteristics of the rock. Interval velocity is calculated using the Dix formula (Baldi et al 2009). The map reveals a more jagged trend with respect to the previous data, with a lower limit of generally 4,000 m/sec, and some circular and concentric shaped zones showing generally lower values (lower than 4,000 m/sec).

Based on the 3D model, a geological profile of the tunnel was published (Fig. 7), indicating:

a) The DSGSD cover occupies a significant part of the upper central zone of the section. Discontinuities and/or secondary slip surfaces have been highlighted within it;
b) The lower DSGSD earth flow (or “bed”) generally affects the “Gneiss di Antigorio” (GA) and also the metasedimentary sequence over a 200 metre thickness. In any case, this surface never reaches or comes close to the altitude of the tunnel;
c) In the “Gneiss di Antigorio” various discontinuities have been revealed;
d) The “metasedimentary sequence” shows a regular pattern although affected by a system of faults, each of which has been assigned an increasing number from south to north, for the purposes of representation and description;
e) The lithotypes pertaining to the “metasedimentary sequence” have been subdivided into different groups where possible, and in particular:
   - *Mma: altered marble;*
   - *Mmp: prevalent marble;*
   - *Me: evaporitic lithotypes in banks and lenses*, present exclusively at the base of the sequence;
f) The base is constituted by the "Micascisti di Baceno" (MB) and is affected by the same system of faults which affects the metasedimentary sequence.

The lower part of the figure from top to bottom shows the following elements:

a) Thickness of the tunnel cover, expressed in metres;
b) Layout of geological structure at the tunnel crown (514.8 m above sea level) and invert (510.0 m above sea level), each for a stretch of 50 metres;

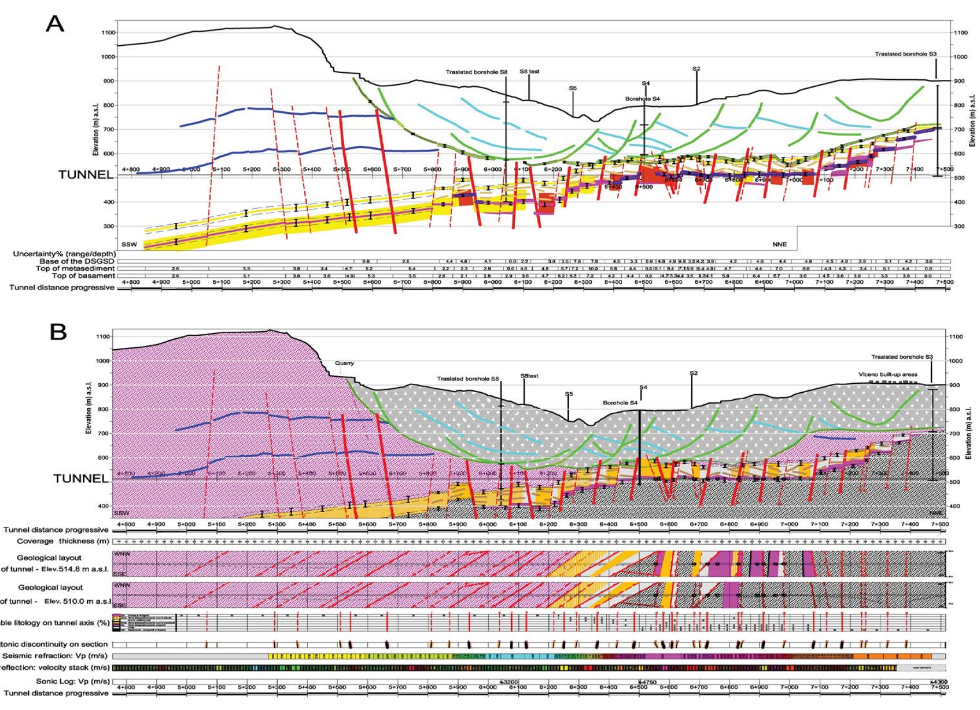

Figure 7. Geophysical (A) and geological-structural (B) models of the tunnel profile.

c) on each side. In these sections the following elements have been reported:
   - Faults are defined as either definite or indefinite with an indication of the lower area;
   - The most probable lithology and the subdivision of various lithotypes for the metasedimentary sequence where possible.

d) The probable lithology on the tunnel axis. Homogenous stretches have been identified, often marked out by faults. Each of these units has been assigned a probability expressed as a percentage, in relation to the possibility that the stretches will be revealed whether independently or associated, at the excavation face. Two sub-units have been derived from the geological interpretation of seismic reflection parameters (interval velocity and complex attributes), defined as mixed and undifferentiated marble.

e) The tectonic discontinuities identified in the section have been defined as either definite or indefinite. Depending on the intensity of the seismic signal and its inclination, each discontinuity has been placed into a geometrical band of uncertainty with a probability range expressed as a percentage between 0 and 100. The dimensions of these bands range between 5, 10 and 15 m.

f) Seismic velocity Vp expressed in m/sec with velocity values accurately measured at of 10 meter intervals and ranging from a minimum of 4,580 to a maximum of 6,990 m/sec.

g) Seismic stacking velocity obtained from seismic reflection, again expressed in m/sec measured at 10 meter intervals and ranging from a minimum of 3,250 to a maximum of 4,870 m/sec.

h) Sonic velocity values, in m/sec, recorded during the three deep geognostic surveys.

Finally in order to simplify the geological model, axonometric reconstruction projections were also prepared (Fig. 8).

In Figure 9 is depicted the three-dimensional geological model based on the high resolution seismic lines and boreholes.

In Figure 9A the top and bottom surfaces of the metasediments are reproduced. In the northern section the top of the basement is constructed by contour lines with an elevation greater than the elevation of the diversion tunnel (510 m a.s.l.). These contour lines highlight the area where the tunnel would always lie below the metasediments, i.e. inside the basement of the Baceno micaschist. The layout of the basement top was also correlated to the same rocks out cropping along Alfenza Creek around 770 m asl and the evidence of an older geoelectric survey (E4 on the map).

In the southern section, the top of the metasediments is reproduced by contour lines below 510 m asl where the tunnel would be excavated in Antigorio gneiss.

The central section of the geological model is horizontal 510 m a.s.l. and corresponds to the tunnel stretch crossing the metasediments. This zone between the basement top and the gneiss base has a mean NE-SW strike in accordance with the general geological setting and a dip toward SE.

In Figure 9B is reproduced the base surface of the DSGSD (Deep Seated Gravitational Slope Deformation). The contours suggest a general sliding direction toward SE.

In Figure 9A are also reported 4 alternative tunnel alignments which maintain the minimum curvature radius of 500 m, minimize the metasediment crossing length, localize the entrance and exit from the metasediments where the gradient of

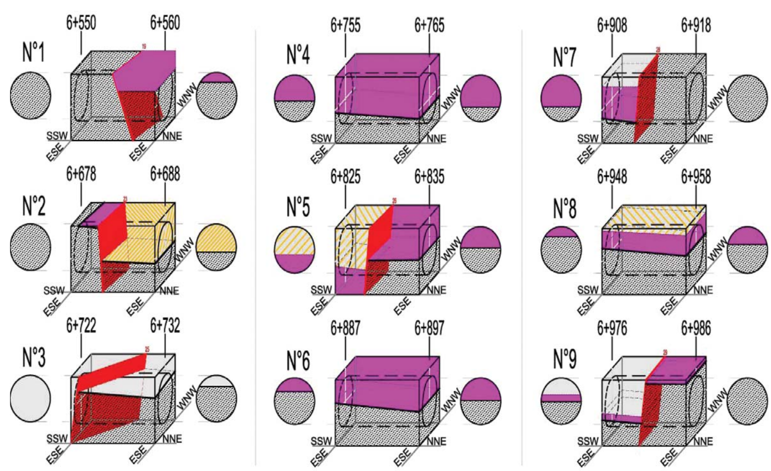

Figure 8. Axonometric projections.

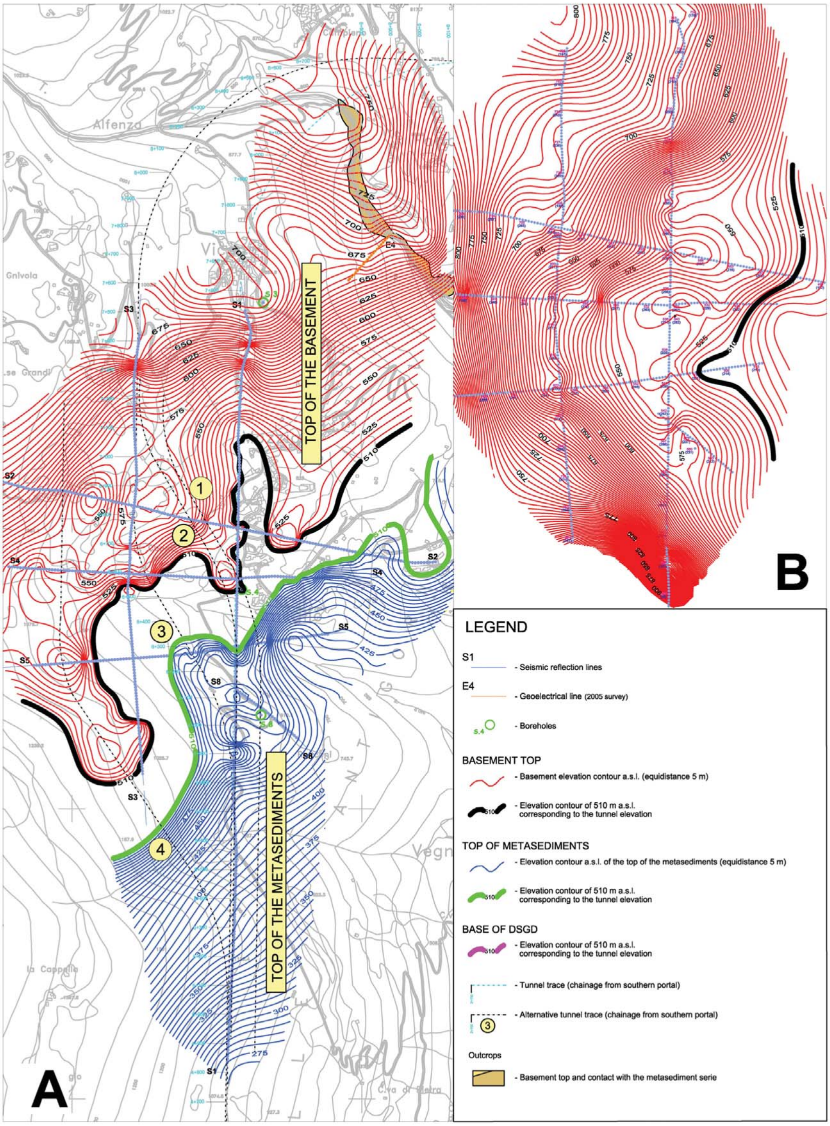

Figure 9. Three-dimensional geological model of the diversion tunnel northern sector. A: Top of basement and metasediment surfaces respectively above and below the tunnel elevation of 510 m a.s.l. Four alternative tunnel traces are indicated. B: map of the DSGSD base highlighting the 510 m a.s.l. contour.

the contact is higher and maximize the separation from the base of the DSGSD.

5 CONCLUSIONS

The geophysical prospecting investigations enabled building a 3D geological model in the area intended for excavation for a future hydraulic tunnel. The model allowed for the different geological units to be positioned in space according to probabilistic and statistical criteria at the various levels along the tunnel excavation. Certain critical situations which will be revealed as tunnelling progresses, were also defined and described.

The model also allowed for various alternate tunnel configurations to be reviewed, which would redacte the length of the critical section of the excavation in the altered lithotypes keeping the tunnel elevation the same.

An analysis of seismic velocities, obtained from both refraction and reflection profiles made it possible to correlate to geomechanical characteristics of the rocks. This will allow for further assessment during the actual excavation, in order to reduce uncertainties, which any tunnel excavation in complex geological conditions would entail.

REFERENCES

Agliardi F., Crosta G., Zanchi A. 2001. Structural constraints on deep-seated slope deformation kinematics. *Engeneering Geology* 59: 83–102.

Badley P. 1988. Practical Seismic Interpretation, P.P.

Baldi A.M., Bianchi F 1999. Sperimentazione della tecnica di rilievo sismico a riflessione T.S.P. per l'esplorazione sull'avanzamento delle gallerie. Atti XX Convegno Nazionale di Geotecnica: "Sviluppi nell'esecuzione e nell'impiego delle Indagini Geotecniche"- Associazione Geotecnica Italiana—Parma .

Baldi A.M., Bianchi F., Boerio V., Francia S., Giorgi F. 2001. New layout of A1 Florence—Bologna highway: integrated seismic rerflection survey and tomographic inversion to perform structural geological modelling along the main tunnel route, Atti Congresso "ITA 2001 Word Tunnel Congress: Progress in tunnelling after 2000", Milano 2001. Ed. Patron, Bologna vol. I, 147–156.

Baldi A.M., Bianchi F., Boerio V., Francia S., Giorgi F. 2001. Construction of third lame aloug the A1 highway across hilly Florence outskirts: geophysical investigation at tunnel routes, Atti Congresso "ITA 2001 Word Tunnel Congress: Progress in tunnelling after 2000", Milano 2001, Ed. Patron Bologna vol. I, 157–167.

Baldi A.M., Bianchi F., Giorgi F., De Marco M., Locatelli E., Ferrari F. 2006. The reconstruct of the geologic section of motorway tunnels with seismic survey: "Connecting road from A4 to Valtrompia" Lumezzane—Brescia. Atti del Congresso "Fifteenth international symposium on Mine Planning & Equipment Selection", Torino. Vol. 1 525–530.

Baldi A.M, Fuoco S., De Luca J. 2006. Application of new seismic methodologies for the solution of geomechanic problems connected to the excavation of tunnels. Atti: fifteenth international symposium on Mine Planning & Equipment Selection. Torino. Vol. 1 531–536.

Baldi A.M., Fuoco S., Cucino P., Nucolussi Paolaz P. 2007. Lo scavo della galleria stradale di Martignano (Trento): previsioni e riscontri, il ruolo delle indagini geofisiche. Atti XXII Convegno Nazionale di Geotecnica ad Abano "Previsioni e controllo del comportamento delle opere". Pàtron Editore, Bologna, 123–130.

Baldi A.M., Ceveneini G., Gambassi R., Notari D. 2009. The processing of interval seismic velocities has allowed, by bulding a statistical-neural, to predefine the time for excavation of gallery with TBM. Atti del workshop in geofisica tenutosi a Rovereto il 25 – 26 giugno 2009: "Nuove frontiere per la geofisica applicata".—Rovereto Ed. Osiride.

Bigioggero B., Boriani A., Origoni Giobbi E. 1977. Microstructure and mineralogy of an Orthogneiss (Antigorio Gneiss—Lepontine Alps). *Rendiconti Società Italiana di Mineralogia e Petrologia* 33:99–108.

Bistacchi A., Massironi M. 2000. Post-nappe brittle tectonics and kinematic evolution of the north-western Alps: an integrated approach. Tectonophysics 327: 267–292.

Bringiotti M. 1996, Guida al Tunnelling. L'arte e la tecnica, Edizioni PEI.

Campani M., Mancktelow N., Seward D., Rolland Y., Müller W., Guerra I. 2010. Geochronological evidence for continuous exhumation through the ductile-brittle transition along a crustal-scale low-angle normal fault: Simplon Fault Zone, central Alps. *Tectonics* 29, TC3002, doi:10.1029/2009TC002582.

Cardarelli E., Bernabini M., De Nardisd R. 1995. Some consideration in travel time tomograpphy in shallow seismic survey. Extended Abstract 57th Conference of EAEG in Glasgow.

Cardarelli E., 2003. Ray Tracing applied to travel time seismic tomography (Theory and examples) Bollettino di geofisica Teorica ed Applicata. Vol. 44 281–305.

Cardarelli E., 2008. Modelling—2D complex anomalies by seismic tomography, (detection and delineation of anomalies with sharp boundaries). Bollettino di geofisica teorica ed Applicata Vol. 49 n. 2 pp. 265–277.

Castiglioni G. 1958. Studio geologico e morfologico del territorio di Baceno e Premia (Val d'Ossola—Alpi Lepontine). *Memorie degli Istituti di Geologia e Mineralogia dell'Università di Padova* XX: 2–82.

Couvreur J.F., Thimus J.F. 1996. Creep and ultrasonic waves. Symposium "Eurock 96" Torino. 41–47.

Feroci M., Orlando L., Balia R.,Bosman C., Cardarelli E., Deidda G., Some considerations on shallow seismic reflection surveys 2000 Journal of Applied Geophysics 45 127–139.

Geophysical Service Inc. 1980. Course of instruction in the geophysics of seismic data processing, Dallas, Texas.

Grasemann B. & Mancktelow N. 1993. Two-dimensional thermal modelling of normal faulting: the Simplon Fault Zone, Central Alps, Switzerland. *Tectonophysics* 225: 155–165.

Grosjean G., Sue C., Burkhard M. 2004. Late Neogene extension in the vicinity of the Simplon fault zone (central Alps, Switzerland). *Eclogae geol. Helv.* 97: 33–46.

Hope V.S., 1993. Application of seismic trasmission tomography in civil engineering. PhD. Dissertation University of Surrey USA.

Hope V.S., Clayton C.R.I., Barla G. 1996. Class "A" predictions of the locations of major rock discontinuities at a storage cavern site, using seismic tomography. Symposium "Eurock 96" Torino. 925–932.

Kaus A., Wolf Boening & Partner GbR 2008. BEAM-Real Time Ground Prediction while Tunnel-Drivage.

Kneib G. 1999. Automatic seismic prediction ahead of the tunnel bore machine, Atti dell'EAGE 61st Conference and Technical Exhibition—Helsinki, Finland, 7–11 June. 4–45.

Mancktelow N.S. 1985. The Simplon line: a major displacement zone in the western Lepontine Alps. *Eclogae Geologicae Helvetiae* 78: 73–96.

Maxelon M. & Mancktelow N.S. 2005. Three-dimensional geometry and tectonostratigraphy of the Pennine zone, Central Alps, Switzerland and Northern Italy. *Earth-Science Reviews* 71: 171–227.

Milnes A.G., Greller M., Müller R. 1981. Sequence and style of major post-nappe structures, Simplon-Pennine Alps. *Journal of Sructural Geology* 3: 411–420.

Mora, P., 1989 Inversion = migration + tomography: Geophysics, 54, 1575–1586.

Schmidt C. & Preiswerk H. 1905. Geologische Karte der Simplongruppe. *Beiträge zur Geologischen Karte der Schweiz,* [N.F.] 26, Spezialkarte No. 48.

Steck A. 2008. Tectonics of the Simplon massif and Lepontine gneiss dome: deformation structures due to collision between the underthrusting European plate and the Adriatic indenter. *Swiss Journal of Geoscience* 101: 515–546.

Sattel G., Frey P., Amberg R. 1992. Prediction ahead of the tunnel face by seismic methods-pilot project in Centovalli Tunnel, Locarno, Switzerland. First Break, January 92, vol. 10.

Sheriff R.E., Geldart L.P. 1976. Structural Interpretation of Seismic Data: Am. Assoc. Of Pet. Geol. Ed. Course note ser. 23.

Tarantola, A., 1988, Theoretical background for the inversion of seismic waveforms, including elasticity and attenuation: in Scattering anda Attenuation of Seismic Waves, Birkhaeuser, Basel.

Zwingmann H. & Mancktelow N. 2004. Timing of Alpine fault gauges. *Earth and Planetary Science Letters* 223: 415–425.